

MR-guided Radiotracer Input Function Estimation in Simultaneous MR/PET

Daniel Burje Chonde^{1,2}, and Ciprian Catana¹

¹Martinos Center for Biomedical Imaging, Charlestown, MA, United States, ²Biophysics, Harvard University, Cambridge, MA, United States

INTRODUCTION: In order to accurately estimate biologically relevant information (e.g. kinetic parameters, binding potentials, cerebral metabolic rate of glucose [CMRglc]) from dynamic PET data, the plasma time activity curve, or input function (IF), is necessary. The gold standard for measuring the IF is through arterial sampling (AIF) performed throughout the PET scan. However, this method is invasive in nature and requires additional research staff [1]. Alternatively, numerous less-invasive methods have been proposed to measure the IF from the PET data directly [2]. These image derived input function (IDIF) methods can solely rely on the PET data or can utilize structural imaging modalities to derive the vasculature. PET-only methods can be subject to bias and noise which can limit their accuracy, especially as it is difficult to differentiate between arteries and veins. Similarly, coregistration of sequentially acquired images for this purpose has been shown to have limited accuracy due to both the lack of mutual information in the vascular regions and deformations of the vasculature due to the different head positions of each scan [3]. Simultaneous MR-PET has the potential to solve this problem as both MR and PET are acquired simultaneously in space and time.

MATERIALS AND METHODS

Integrated MR-PET Scanner: The BrainPET, a MR-compatible brain PET scanner prototype installed at our site, was used for these experiments. This system operates while inserted into the bore of the Siemens 3T TIM Trio MR scanner [4].

MR Acquisition: Time-of-flight (TOF) angiography ($0.7 \times 0.5 \times 0.7 \text{ mm}^3$, TR/TE=24/3.68 ms, FA=18°, TA=6:16 min) was acquired along with ME-MPRAGE (1mm³ isotropic, TR/TI/TE = 2530/1200/1.64 ms, FA=7°, TA=4:56 min) during simultaneous MR-PET imaging.

Arterial Mask Generation: To generate the arterial mask, first the TOF and ME-MPRAGE volumes were moved to isocenter. Due to intensity inhomogeneities in the TOF data and slab boundary artifacts, simple thresholding does not yield accurate arterial segmentation; rather, the TOF images first underwent morphologic top-hat filtering. A high threshold was applied to a rectangular region in the center of the TOF volume to capture some arterial segments. These segments were then used as a seed for a region-growing algorithm. To extend the mask into the carotid region, the TOF derived mask was used as a seed for another region growing algorithm with the MPRAGE as the image volume. To prevent growing into high intensity regions in the MPRAGE which did not correspond to vasculature (e.g. edematous regions in brain tumor subjects), the portion of the head which is included in both the TOF and MPRAGE images is excluded from the MPRAGE region growing step except for a small overlap which is necessary to allow the region to grow.

Effect of Motion on Mask Generation: To explore the effects of patient motion on the mask, TOF and MPRAGE MR images were acquired in 5 positions. The TOF images were coregistered to a reference position and the offsets were applied to the MPRAGE. Arterial mask generation was performed on the "motion corrected" TOF/MPRAGE pairs. The preservation of structure was determined.

Data Acquisition Protocol: To validate our model, PET and MR data were simultaneously acquired in human subjects continuously for at least 60 minutes. Prior to imaging, an arterial line was placed in the radial artery to allow for sampling of arterial blood throughout the scan. The subject was then placed inside the MR-PET and dynamic FDG-PET imaging was performed. Arterial blood samples were collected every 5 seconds for the first two minutes after injection and then at 5, 10, 15, 20, 30, 45, 60, 75, and 90 minutes post injection. The PET data was acquired in list mode format and subsequently binned into 12x5sec, 2x30sec, 3x60 sec, 2x150 sec, 2x300 sec, 7x600 sec frames. The frames were reconstructed using a 3D-OPOSEM algorithm and corrections were applied to account for variable detector efficiency and deadtime, random coincidences, photon attenuation, and scatter. All of the reconstructed images were decay corrected to the time of injection. To derive the IDIF, the dynamic PET imaging series was used and partial volume corrections were applied using an adaptation of Chen's method [1].

RESULTS AND DISCUSSIONS

Arterial Mask Generation: MR TOF is capable of resolving both large and small arterial structures using bright-blood techniques (Fig 1.A); however, for extended fields of view (FOV) it can be quite time consuming. ME-MPRAGE, which is faster and is commonly acquired for anatomical correlation between MR and PET, also exhibits a hyper-intense arterial blood signal in larger vessels (Fig 1.B). The combined TOF and MPRAGE method for arterial mask generation provided a continuous mask which accurately segmented both large and small vessels, and reduced scan time. This arterial mask (Fig 1.C) can then be applied as an ROI to dynamic PET images (Fig 1.D) to derive an IDIF.

Effect of Motion on Mask Generation: No visible deformations in the arterial mask were noted; however, the small vessel areas showed less preservation than the large vessels. This decreased preservation is likely a result of the algorithm as its performance in segmenting smaller vessels is best when the subject's head is aligned with the B_0 field.

IDIF: Similar to Chen's findings, we observed an over estimation in the IDIF peak value [1]. Using a shape-preserving spline, the area under the curve (AUC) of the IDIF was found to be $95.2\% \pm 2.6\%$ of the AIF with an RMS error of 0.42 ± 0.14 SUV. It has been shown that improper estimation of the peak using Chen's method can still provide accurate estimation of CMRglc [1,5,6]. Manually placed VOIs around the Putamen observed an increase in CMRglc on the order of $1.55\% \pm 0.23\%$ when using the IDIF as compared to the AIF. A possible explanation for the discrepancy between the IDIF and AIF peak and shape is that the IDIF achieves a higher temporal resolution than that of arterial sampling which is approximate. To further explore this and to validate our method we are in the process of building an MR-compatible blood sampler which will be capable of high-temporal arterial sampling.

CONCLUSION: We present a novel approach to segment both the large and small vessels from MR images for use in estimation of the IDIF. Unlike sequential MR and PET, our masks are unaffected to registration errors and are robust to patient motion.

REFERENCES: [1] Chen K et al, J Cereb Blood Flow Metab, 1998; 18: 716-723. [2] Zanotti-Fregonara P et al, J Cereb Blood Flow Metab, 2011; 31: 1986-98. [3] Fung EK et al, IEEE Nucl Sci Symp Conf Rec, 1997; 2710-4. [4] Schlemmer HP et al, Radiol, 2008; 248(3):1028-35. [5] Zanotti-Fregonara P et al, PLoS One, 2011; 6(2): e17056. [6] Zanotti-Fregonara P et al, J Cereb Blood Flow Metab, 2009; 29: 1825-35.

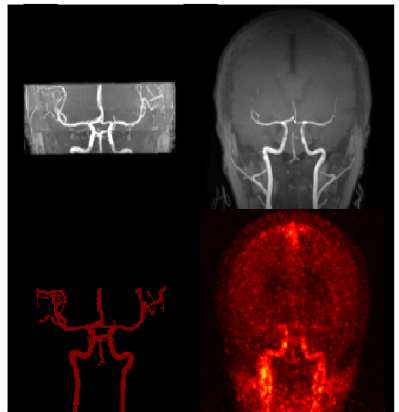


Fig 1: Combining high resolution arterial detail of TOF MR (A) and large FOV of MPRAGE (B) allows for the construction of an arterial mask (C) which includes both large and small arteries which can be used to generate an IDIF for PET (D). All images are MIPs of central 50 slices.

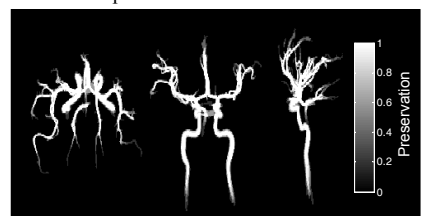


Fig 2: The arterial mask preservation with regard to motion as derived from a healthy volunteer, shown in MIP, displays that even in the presence of head motion the arterial structures remain undeformed in the MR-PET head coil.

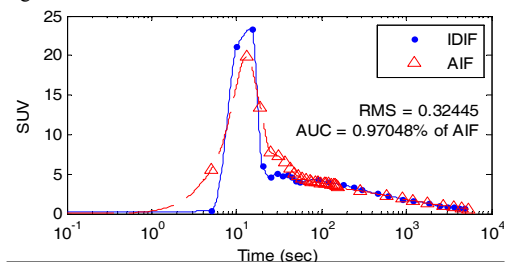


Fig 3: Representative IDIF compared to AIF. While Chen's PVC method leads to an over estimation in the peak intensity, there is excellent agreement with later time points.